NON-REFLECTIVE MICROWAVE FREQUENCY-SELECTIVE CIRCUITS BASED ON COUPLED STRIPLINES AND LUMPED RLC-ELEMENTS AND THERE APPLICATION

N.D. Malyutin, G.A. Malyutin

Tomsk State University of Control Systems and Radioelectronics
40 Lenin Ave., Tomsk, 634050 Russian Federation
E-mail: ndm@main.tusur.ru

Abstract: *Non-reflecting frequency-selective circuits (NFSC) based on coupled strip lines (CSL) and lumped RLC-elements are investigated. The frequency characteristics of NFSC are analyzed for known design parameters of CSL, and parameters of RLC-elements. It is shown that the use of the proposed circuits containing a section of coupled lines, the diagonal ports of which are loaded with the impedance of RLC circuits on lumped elements, makes it possible to obtain the frequency response of a bandpass filter with a minimum reflection coefficient from the input and output in a single passband and stopbands in a wide frequency range. The inverse problem of determining the impedance of RLC circuits from lumped elements based on a given scattering matrix of the NFSC has been solved. The parameters of non-reflecting filters based on the proposed circuits have been experimentally confirmed: losses of –2.1 dB at a central frequency of 949.2 MHz of a passband of 174.1 MHz; return losses of no more than – 10 dB up to a frequency of 7.5 GHz in the entire frequency range.*

Keywords: *coupled strip lines, non-reflective bandpass filter, lumped elements, RLC-circuit, frequency characteristics.*

1. Introduction

Combining the property of frequency selectivity and minimal reflection in a wide frequency band is a non-trivial task. The solution to this problem opens up new possibilities for designing non-reflective filters, amplitude correctors and other devices. The problem is that when designing bandpass filters based on coupled lines, we obtain in the stop band a reflection coefficient S_{11} close to unity. The presence of reflections at out-of-band frequencies can lead to the occurrence of intermodulation distortions in the equipment. As is known, return losses determine the portion of signal power that does not enter the device due to signal reflection from its input. Losses of microwave power conversion into heat due to finite conductivity of conductors and imperfection of dielectrics are considered undesirable, worsening the quality of the band-pass properties of the circuit and, in particular, band-pass filters. The presence of signal reflections at out-of-band frequencies is undesirable in a number of cases. This applies to multichannel systems, to circuits containing nonlinear elements. Therefore, the direction of creating non-reflective filters, which are also called absorption filters, has recently begun to develop [1]. If the reflection coefficient in the rejection band $S_{11}^{\mathbf{H}}$ is chosen as the criterion, then the variety of microwave circuits can be divided into two types: microwave reflective circuits (RC) with reflection coefficient $S_{11}^{\mathbf{H}} \to 1$; non-reflective circuits (NC) with reflection coefficient $S_{11}^{\mathbf{H}} \to 0$.

Reflective circuits are built based on high-quality resonators formed by sections of strip lines and coupled strip lines (CSL).

Non-reflective circuits, as well as RCs, can be divided according to the use of distributed and lumped elements:

1) NCs based on lumped RLC elements [2];

2) NCs based on sections of loaded strip lines [3];

3) NCs including coupled strip lines (CSL) [4].

In this paper, we consider non-reflective microwave circuits based on CSL and lumped RLC-elements. The goal is to solve the problem of modeling non-reflective frequency-selective circuits with the proposed structural diagram for given design parameters of the CSL and different RLC circuits.

The problem of finding the frequency dependence of the impedance of RLC circuits, necessary for implementing the required frequency dependence of the transmission coefficient and reflection coefficient of non-reflective circuits, is solved using non-reflective filters as an example.

1. Designs of microwave devices and their equivalent circuits in the form of non-reflective circuits

Fig. 1 shows a three-dimensional model of a device on coupled strip lines with the inclusion of concentrated RLC elements.

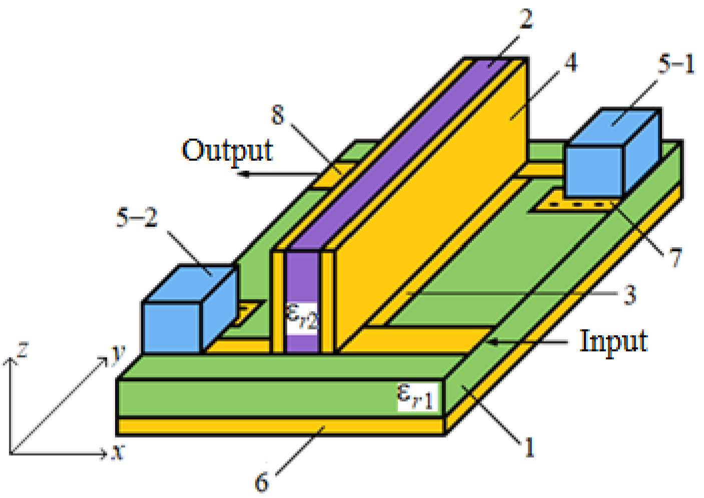

Fig. 1. Three-dimensional model of NFSC on CSL 3D-design

The coupled lines are formed by connecting horizontal and vertical strips 1 and 2. The latter are obtained by installing a vertical dielectric substrate 3 metal-lized on both sides. Frequency-dependent loads in the form of RLC circuits 4-1 and 4-2 are connected to the diagonal arms through connecting strips 5 and are grounded on contact pads 6. To increase the self-capacitances of the horizontal conductors, substrate 1 is equipped with a grounded base 8 on the reverse side.

The equivalent circuit of the NBPF is shown in Fig. 1, b with the designated length of the CSL l.

Its feature is the use of coupled strip lines made on horizontal and vertical substrates with different relative permittivities $\boldsymbol{\varepsilon}_{r1}$ and $\boldsymbol{\varepsilon}_{r2}$ [5]. The coupled strip lines section of the CSL in the general case with an unbalanced electromagnetic coupling [6].

Since the transverse dimensions of the vertically and horizontally located strips are much smaller in relation to the wavelength at the frequencies used up to 8 GHz, it is advisable to model the device under the assumption of the existence of quasi-transverse electromagnetic waves, or quasi-T-waves, in them [7]. Therefore, the equivalent circuit of the non-reflecting device is presented in 2D dimension (Fig. 2). It is obtained by decomposing the design (Fig. 1) into its component parts, each of which is represented as an eight-terminal network.

Unequal coupled strip lines I and II with unbalanced electromagnetic coupling are separated into block ***A***, called the distributed element block. Blocks ***B***1 and ***B***2 consist of concentrated RLC circuits. The circuit in the form of a cascade connection of three eight-terminal devices is convenient for analysis, since the NF transfer matrix in this case is a product of matrices $\mathbf{a}_{B1}$, $\mathbf{a}$, $\mathbf{a}_{B2}$ [8].

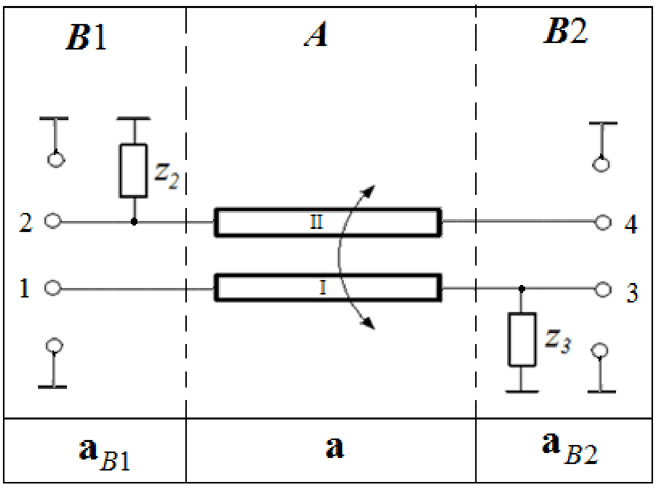

Fig. 2. Equivalent circuit of a non-reflective strip filter as an eight-port network: ***A*** is a block of a distributed structure of coupled lines I, II; ***B***1, ***B2*** are blocks of lumped RLC circuits; A is the transmission matrix of an eight-port network composed of coupled lines I and II; $\mathbf{a}$ are transmission matrices of eight-port networks describing the inclusion of RLC circuits

When the device is connected to the circuit, only ports 1 and 4 are used. In this case, the device is a four-terminal device, derived from a multi-terminal device formed by blocks ***B***1, ***A***, and ***B***2. Detailing the decomposition of block ***A***, as well as blocks ***B***1, ***B***2, allows us to take into account the influence of the constituent elements of the blocks on the characteristics of the circuit.

2. Modeling of non-reflective circuits

The equivalent circuit for block ***A*** implemented as a section of coupled strip lines I and II of length l (Fig. 1), blocks ***B***1 and ***B***2 as RLC circuits containing series oscillatory circuits with inductances *L*01, *L*02, capacitances *C*01, *C*02, shunt resistances *R*01, *R*02, is simplified to the form shown in Fig. 3. We will consider this circuit as a base for studying the main properties of non-reflective circuits depending on the parameters of the CSL and the parameters of the RLC elements of blocks ***B***1 and ***B***2.

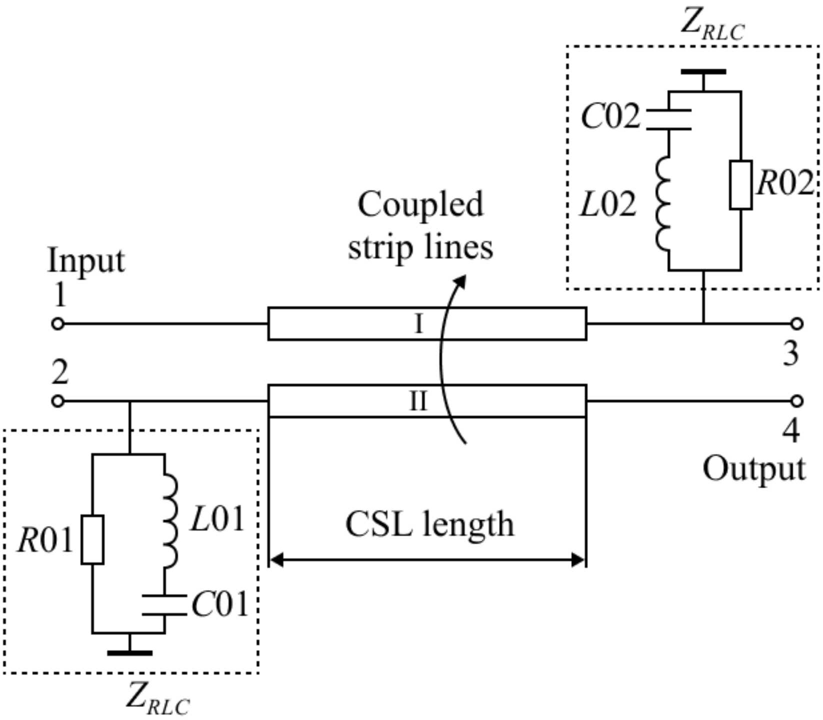

Fig. 3. Equivalent circuit of the basic version of non-reflective circuits in the form of a four-terminal network, derived from an eight-terminal network (Fig. 2)

We will construct a model for analyzing the NFSC based on an equivalent circuit in the form of a cascade connection of eight-terminal networks (Fig. 2) with a subsequent transition to a circuit of a non-reflective frequency-selective circuit in the form of a four-terminal network (Fig. 3).

It is assumed that the input and output (ports 1 and 4) are loaded with the resistances of external devices z_1 and z_4, usually 50 Ohm. The loads in ports 2 and 3 are RLC circuits with different impedances z_1 and z_4. When NFSC is included in the equipment, external ports 2 and 3 are not used, they are only needed when analyzing the circuit in Fig. 2.

The transfer matrix of the NFSC as an eight-terminal network formed by a cascade connection of eight-terminal networks $\mathbf{a}_{B1}$, $\mathbf{a}$, $\mathbf{a}_{B2}$ is in the form of a product $\mathbf{a}_\Sigma = \mathbf{a}_{B1} \times \mathbf{a} \times \mathbf{a}_{B2}$ [27]. By multiplying the matrices, we obtain the transfer matrix of the structural circuit under consideration in Fig. 2

$$\mathbf{a}_\Sigma = \left[\mathbf{a}_{\Sigma 1} \quad \mathbf{a}_{\Sigma 2} \quad \mathbf{a}_{\Sigma 3} \quad \mathbf{a}_{\Sigma 4}\right], \tag{1}$$

in which the submatrices $\mathbf{a}_{\Sigma 1},\dots,\mathbf{a}_{\Sigma 4}$ are determined from the following formulas (2)

$$\mathbf{a}_{\Sigma 1} = \begin{bmatrix} a_{11} + a_{13} \cdot z_3^{-1} \\ a_{21} + a_{14} \cdot z_3^{-1} \\ a_{31} + a_{11} \cdot z_3^{-1} \\ a_{32} + \left(a_{12} + a_{14} \cdot z_2^{-1}\right) \cdot z_3^{-1} + a_{21} \cdot z_2^{-1} \end{bmatrix}, \qquad \mathbf{a}_{\Sigma 2} = \begin{bmatrix} a_{12} \\ a_{22} \\ a_{32} \\ a_{42} + a_{22} \cdot z_2^{-1} \end{bmatrix},$$

$$\mathbf{a}_{\Sigma 3} = \begin{bmatrix} a_{13} \\ a_{13} \\ a_{11} \\ a_{12} + a_{14} \cdot z_2^{-1} \end{bmatrix}, \qquad \mathbf{a}_{\Sigma 4} = \begin{bmatrix} a_{14} \\ a_{24} \\ a_{21} \\ a_{22} + a_{24} \cdot z_2^{-1} \end{bmatrix}, \tag{2}$$

where a_{ij} $(i, j = 1,\dots,4)$ are the elements of the matrix of coupled strip lines.

Matrices $\mathbf{a}_{B1}$, $\mathbf{a}_{B2}$ are defined in [8], the matrix $\mathbf{a}$ of coupled strip lines for the most general case of unequal lines with non-uniform dielectric filling are calculated according to [6, 9].

Input port 1 and output port 4 in the non-reflective circuit are loaded with resistances z_1, z_4, and ports 2 and 3 are not used. Therefore, from the eight-terminal circuit (Fig. 2) we can move to the derivative four-terminal circuit [8] with the transfer matrix, which is the circuit in Fig. 3. Because of this transition, we obtain $\hat{\mathbf{a}}$ 2×2 matrix that relates the input voltage and current to the output voltage and current. Its coefficients are found as follows

$$\begin{aligned} \hat{a}_{11} &= [a_{12} \cdot \boldsymbol{\varphi} - \boldsymbol{\beta} \cdot (a_{22} + a_{24} \cdot z_2^{-1})] \cdot \Delta^{-1}, \\ \hat{a}_{12} &= [a_{14} \cdot \boldsymbol{\varphi} - \boldsymbol{\beta} \cdot (a_{42} + a_{22} \cdot z_2^{-1})] \cdot \Delta^{-1}, \\ \hat{a}_{21} &= [a_{32} \cdot \boldsymbol{\varphi} - \boldsymbol{\eta} \cdot (a_{42} + a_{22} \cdot z_2^{-1})] \cdot \Delta^{-1}, \\ \hat{a}_{22} &= [a_{21} \cdot \boldsymbol{\varphi} - \boldsymbol{\eta} \cdot (a_{22} + a_{24} \cdot z_2^{-1})] \cdot \Delta^{-1}, \end{aligned} \tag{3}$$

where $\boldsymbol{\varphi} = a_{32} + z_3^{-1} \cdot (a_{12} + a_{14} \cdot z_2^{-1}) + a_{21} \cdot z_2^{-1}$, $\boldsymbol{\beta} = a_{11} + a_{12} \cdot z_3^{-1}$, $\eta = a_{31} + a_{11} \cdot z_3^{-1}$, $\Delta = a_{32} + z_1^{-1} \cdot (a_{12} + a_{14} \cdot z_2^{-1}) + a_{21} \cdot z_2^{-1}$.

Thus, the matrix $\mathbf{\hat{a}}$ obtained from expressions (3) represents an analytical model of the NFSC with asymmetric loads in ports 2 and 3. The transition from the description of the NFSC in the form of a transmission matrix $\mathbf{\hat{a}}$ to a scattering matrix [8] makes it possible to calculate the frequency characteristics of non-reflective filters depending on the parameters of the RLC circuits and coupled strip lines.

To check the adequacy of the proposed analytical model, a comparative numerical simulation of the NFSC layout was carried out using the CAD system and a program in the Mathcad mathematical modeling environment, developed on the basis of the presented model. Electrodynamic simulation using CAD was carried out using a 3D model (Fig. 1).

In the calculation using the developed program, the design of coupled strip lines of the VIP type was taken [10]. The cross-section of the CSL is shown in Fig. 4a. Horizontal strips with a width of $w_1 = 0.6$ mm are located on a substrate made of FR4 material with a thickness of $h_1 = 1.5$ mm and a relative permittivity of $\varepsilon_{r1} = 4.5$. The vertical stripes of width $w_2 = 2.0$ mm are made on a vertically installed substrate made of RO-3003 material of thickness $h_2 =$ 0.635 mm. The horizontal conductors of the SPL have a length of $l = 45$ mm.

The parameters of the RLC circuit elements (Fig. 3) were as follows: $C01 = C02 = 1.2$ pF, $L01 = L02 = 23.5$ nH, $R01 = R02 = 50$ Ohm. The calculated frequency dependences of the transmission coefficient $|S_{21}|$ and reflection coefficient (return losses) $|S_{11}|$ of the NFSC are shown in Fig. 4b.

The results of calculations using CAD and the developed program are close, therefore, it is advisable to use modeling in the quasi-T approximation to study the dependences of the parameters of non-reflecting filters on the primary and modal parameters of the CSL, as well as on the frequency properties of the RLC circuits, since the time spent on analyzing one version of the NFSC design is less than a minute.

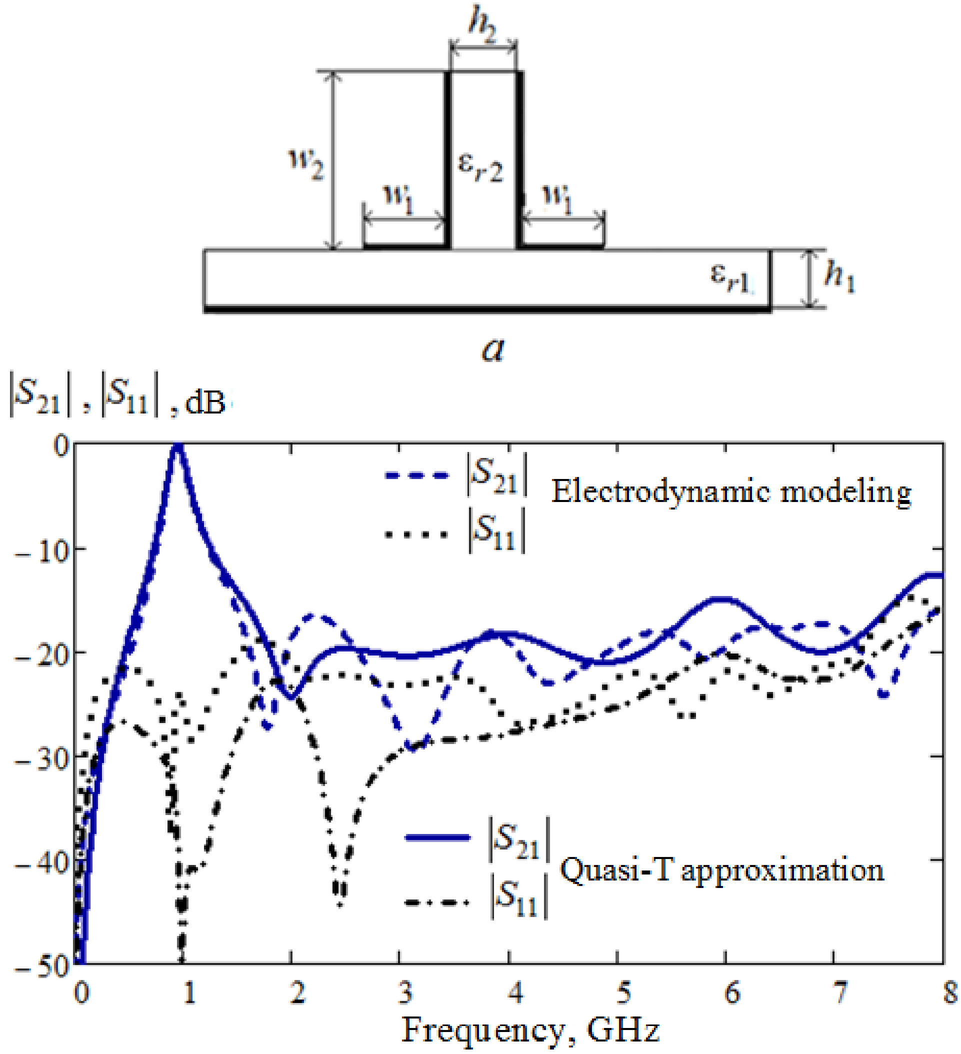

Fig. 4. Cross-section of coupled striplines (a), frequency dependence of transmission coefficient $|S_{21}|$ and reflection coefficient $|S_{11}|$ (b), obtained by electrodynamic modeling and quasi-T approximation

The constructed model was also used, which is especially important, to solve the inverse problem of finding the parameters of the constituent RLC elements of the NFSC for given frequency characteristics.

3. Solution of the inverse problem

When designing filters, the coefficients of the scattering matrix of the device are usually specified as the initial data, and the sought parameters are the characteristics of the main elements of the design and circuit. Therefore, it is necessary to solve the inverse problem. We will use the fact that the existing connection $\hat{\mathbf{a}}$ and $\mathbf{s}$ [8] allows us to find the transmission matrix in a given frequency range for a given complex transmission coefficient S_{21} and complex reflection coefficient S_{11}.

If the design of the coupled lines is determined, then it is easy to calculate using the works [6, 9]. By analogy with [11], with a known matrix **a** and the matrix $\hat{\mathbf{a}}$ being determined, a system of equations is compiled to find z_2 and z_3. Omitting the intermediate calculations, we present expression (4) for calculating the frequency dependence of z_2 and z_3 , written in matrix form

$$\begin{pmatrix} z_2^{-1} \\ z_3^{-1} \\ 2 \cdot z_2^{-1} \cdot z_3^{-1} \end{pmatrix} = \begin{pmatrix} m2 & m3 & m4 \\ m6 & m7 & m8 \\ m10+m14 & m11+m15 & m12+m16 \end{pmatrix}^{-1} \cdot \begin{pmatrix} -m1 \\ -m5 \\ -m9-m13 \end{pmatrix}, \quad (4)$$

where

$$m1 = \hat{a}_{11} \cdot a_{41} - (a_{12} \cdot a_{41} - a_{11} \cdot a_{42}),\ m9 = \hat{a}_{21} \cdot a_{41} - (a_{32} \cdot a_{41} - a_{31} \cdot a_{42}),$$
$$m2 = \hat{a}_{11} \cdot a_{21} - (a_{12} \cdot a_{21} - a_{11} \cdot a_{22}),$$
$$m10 = \hat{a}_{21} \cdot a_{21} - (a_{21} \cdot a_{32} - a_{22} \cdot a_{31}),$$

$$m3 = \hat{a}_{11} \cdot a_{43} - (a_{12} \cdot a_{43} - a_{13} \cdot a_{42}),$$
$$m11 = \hat{a}_{21} \cdot a_{43} - (a_{32} \cdot a_{43} - a_{33} \cdot a_{42}),$$

$$m4 = \hat{a}_{11} \cdot a_{23} - (a_{12} \cdot a_{23} - a_{13} \cdot a_{22}),$$
$$m12 = \hat{a}_{21} \cdot a_{23} - (a_{23} \cdot a_{32} - a_{22} \cdot a_{33}),$$

$$m5 = \hat{a}_{12} \cdot a_{41} - (a_{14} \cdot a_{41} - a_{11} \cdot a_{44}),$$
$$m13 = \hat{a}_{22} \cdot a_{41} - (a_{41} \cdot a_{34} - a_{31} \cdot a_{44}),$$

$$m6 = \hat{a}_{12} \cdot a_{21} - (a_{21} \cdot a_{14} - a_{11} \cdot a_{24}),$$
$$m14 = \hat{a}_{22} \cdot a_{21} - (a_{21} \cdot a_{34} - a_{31} \cdot a_{24}),$$

$$m7 = \hat{a}_{12} \cdot a_{43} - (a_{14} \cdot a_{43} - a_{13} \cdot a_{44}),$$
$$m15 = \hat{a}_{22} \cdot a_{43} - (a_{34} \cdot a_{43} - a_{33} \cdot a_{44}),$$

$$m8 = \hat{a}_{12} \cdot a_{23} - (a_{14} \cdot a_{23} - a_{13} \cdot a_{44}),$$
$$m16 = \hat{a}_{22} \cdot a_{23} - (a_{23} \cdot a_{34} - a_{24} \cdot a_{33});$$

$\hat{a}_{km}\ (k,m=1,2)$ – elements of the transfer matrix of the derivative of the quadrupole, determined from (3) or as a result of the transition from a given matrix **s** to the matrix $\hat{\mathbf{a}}$;

$a_{ij}\ (k,m=1...4)$– elements of the transfer matrix of a segment of coupled strip lines.

The problem of determining z_2 and z_3, which is the inverse problem, significantly accelerates the determination of the parameters of RLC circuits. As already noted, the initial data for its solution are the coefficients of the transmission matrix of the non-reflecting filter and the associated strip lines, which can be obtained by mathematical modeling or experimentally.

4. Experimental results. Extraction of RLC circuit parameters

A model of a non-reflective stripline filter (Fig. 5a) was manufactured based on the circuit under consideration, including a section of coupled striplines (a block with distributed parameters) and an RLC circuit in the form of series oscillatory LC circuits damped by resistance R0. The NFSC is tuned to a central frequency of $f_0 = 0.949$ GHz.

In the calculation, the inductance of $L0 = 22.0$ nH, capacitance of $C0 = 1.2$ pF, and resistance of $R0 = 50$ Ohm were included in the composition of identical RLC circuits. The length of the segment of coupled lines was $l = \mathbf{0.048}$ m. The matrices of linear capacitances $\mathbf{C}$ and inductances $\mathbf{L}$ of the CSL were calculated using the grid method [10] and amounted to

$$\mathbf{C} = \begin{bmatrix} \mathbf{169.7} & \mathbf{-117.4} \\ \mathbf{-117.4} & \mathbf{169.7} \end{bmatrix} \text{ pF/m}, \; \mathbf{L} = \begin{bmatrix} \mathbf{0.3953} & \mathbf{0.2633} \\ \mathbf{0.2633} & \mathbf{0.3953} \end{bmatrix} \; \mu\text{H/m}.$$

Fig. 5b shows a comparison of the results of experimental measurements and modeling in the quasi-T-approximation of the frequency dependence of the transmission coefficient $|S_{21}|$, reflection coefficient $|S_{11}|$. Fig. 6 shows the results of modeling and measuring the group delay time $\tau_{\mathbf{gd}}$ of the manufactured model of a non-reflective filter.

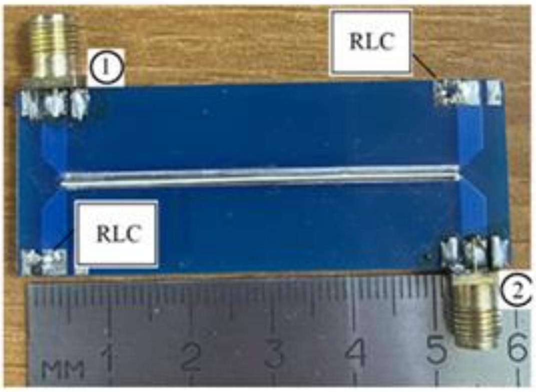

a

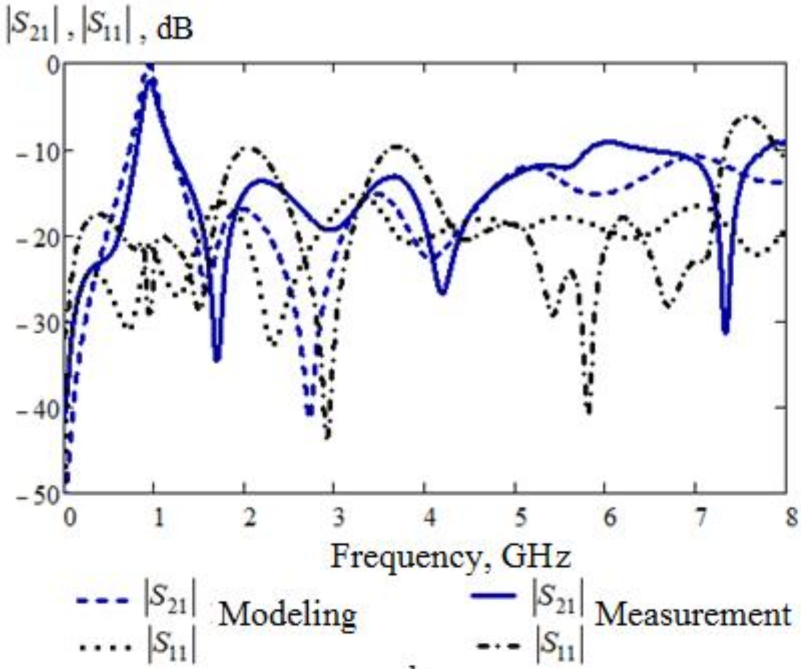

b

Fig. 5. External appearance of the layout of the strip non-reflective band-pass filter (*a*) and the results of modeling and measuring the frequency dependences S_{11}, S_{21}(*b*)

As can be seen from Fig. 5b, the frequency dependences are close to the calculated characteristics of the LFIC in the passband and are qualitatively consistent in the stopbands up to 8 GHz. In the process of modeling according to the obtained relations (2)–(4), it was found that the greatest sensitivity of the frequency characteristics of the NFSC is observed due to the asymmetry of the frequency dependences of the impedances and RLC circuits and the imbalance of the electromagnetic coupling of the coupled striplines, expressed through the coefficients of capacitive coupling and inductive coupling.

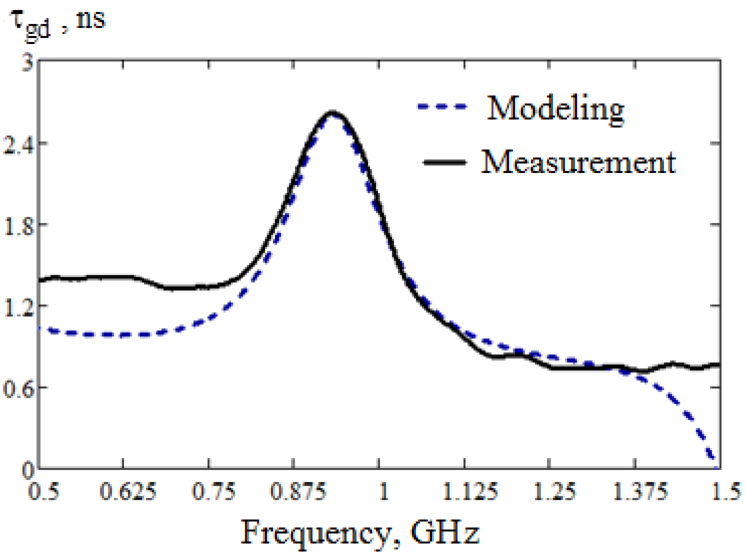

Fig. 6. Frequency dependences of the group delay time $\tau_{\mathbf{gd}}$ of the NFSC layout

In the example considered $k_C = \mathbf{0.692}$, $k_L = \mathbf{0.666}$. With such ratios and at the central frequency of the passband, $|S_{21}(f_0)| = -2.115$ dB, $|S_{11}(f)|$ was experimentally obtained, and outside the passband up to 7 GHz, it is limited to –10 dB.

It should be noted that with known parameters of the coupled lines in the form of a transmission matrix and unknown parameters of the RLC circuits, the obtained solution (4) for finding the frequency dependence allows extraction to be carried out by measuring the scattering matrix of the filter as a four-terminal network and the transition from to the transmission matrix.

In this case, all coefficients become $m1,...,m16$ known and (4) provides a solution to the extraction problem $z_2(f)$ and $z_3(f)$. As an example, Fig. 7 shows the frequency dependences of the impedance moduli of RLC circuits $|z_2|$, $\sqrt{|z_2| \cdot |z_3|}$ obtained from (4) as a result of using the experimental frequency dependences of the scattering matrix coefficients of the NFSC (their frequency dependences are shown in Fig. 5b).

The obtained frequency characteristics allow us to unambiguously reconstruct the parameters of RLC circuits in the form of a series oscillatory circuit shunted by a 50 Ohm resistance.

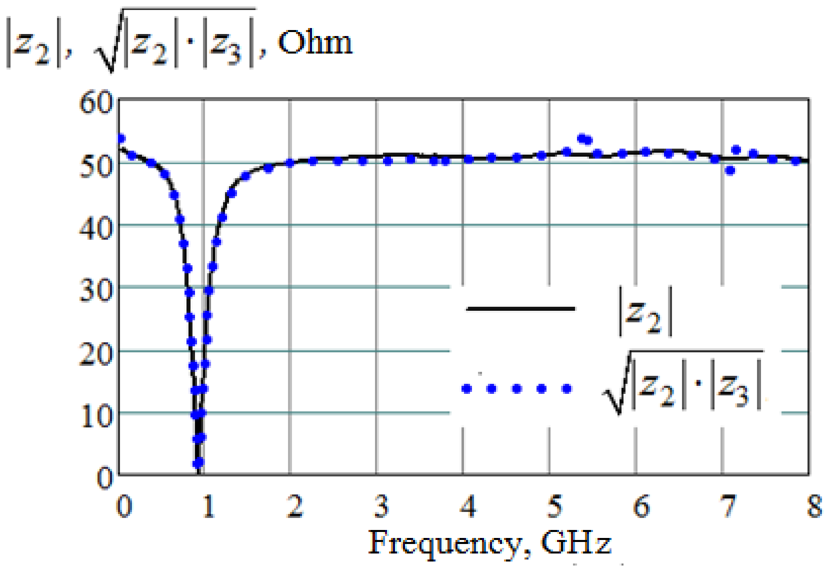

Fig. 7. Reconstructed frequency dependencies $|z_2|$, $\sqrt{|z_2|\cdot|z_3|}$ of RLC circuits

The detailed reconstruction of the parameters of the RLC circuit elements is carried out on the basis of the theory of lumped circuits, which significantly simplifies the synthesis of non-reflective strip filters with the proposed structure.

The frequency dependences of the transfer coefficient $|S_{21}|$ (Fig. 5) and the impedance modulus of the RLC circuit (Fig. 7) indicate the relationship between these characteristics. The maximum $|S_{21}|$ is observed at the resonance frequency $f_0 = \dfrac{1}{2\boldsymbol{\pi}} \cdot \sqrt{(L0 \cdot C0)^{-1}}$ of the series circuit (see Fig. 1), and the first minimum at $f > f_0$ at a frequency f_{01}, corresponds to the electrical length $\boldsymbol{\theta} = (\boldsymbol{\theta}_e + \boldsymbol{\theta}_o)/2 \simeq 180^\circ$ of the coupled lines , where $\boldsymbol{\theta}_e$, $\boldsymbol{\theta}_o$ are the electrical lengths of the strips for the in-phase and antiphase waves.

The frequency characteristics of the NFSC were calculated for different physical lengths of the SPL (Fig. 8). This figure shows the frequency dependence of the transmission coefficient S_{21} of the NFSC, the length of the strips in which varies from 25 mm to 55 mm. A slight influence of the length l of the coupled strips on the frequency f_0 is visible, but as the length l decreases, the frequency f_{01} increases.

From the given dependence, it can be concluded that the central frequency of the passband in the proposed design and scheme of the non-reflective filter is not determined by the length of the sections of the coupled lines, it is determined by the parameters of the RLC circuit (see formulas (5) and (6)). At the same time, the position of the minimum S_{21} in the RLC circuit shown in Fig. 1 is determined by the length l of the strips under the condition $\boldsymbol{\theta} = (\boldsymbol{\theta}_e + \boldsymbol{\theta}_o)/2 \simeq 180^\circ$.

This is precisely the fundamental difference between the proposed solution and traditional filters on coupled strip lines.

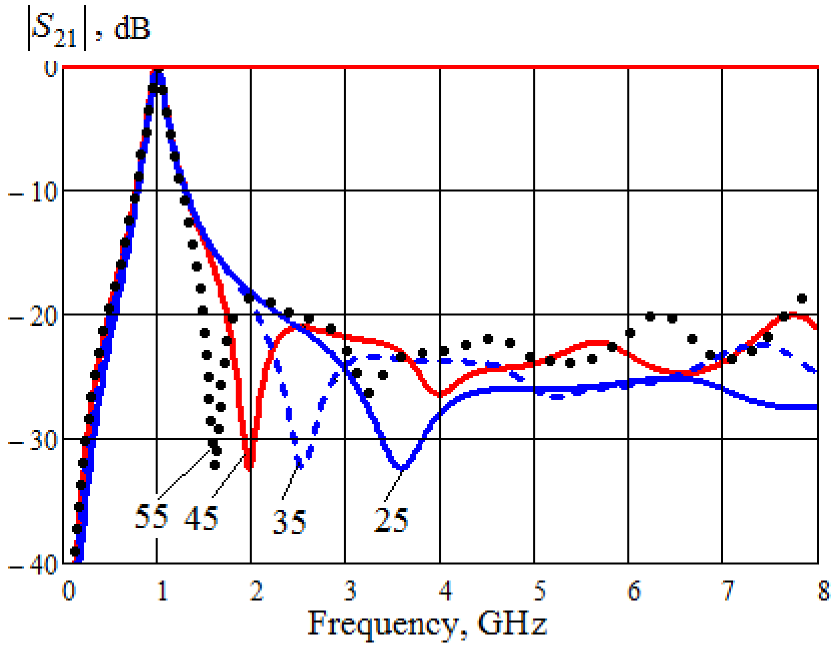

Fig. 8. Frequency dependence of the transmission coefficient of the NFSC, the length l of the connected strips in which varies from 25 mm to 55 mm

5. Conclusion

Thus, the problems of analysis, synthesis and experimental study of non-reflective stripline bandpass filters have been solved. The mechanism of formation of the frequency characteristic of the NFSC is shown, consisting in the transformation of the frequency dependence of the load impedance in the form of an RLC circuit on lumped elements into the antipode of this characteristic using the proposed NFSC scheme. In this case, bandpass filters containing a distributed base element in the form of coupled lines have a single passband and return losses at the level of –10 dB at out-of-band frequencies. It is shown that in the case when the matrix $\mathbf{s}$ is obtained experimentally, the developed algorithm make it possible to extract the frequency dependence of the impedance of the RLC circuit with unknown parameters of the elements included in it. Further studies of frequency-selective devices containing coupled lines and lumped RLC circuits are relevant in the direction of expanding the functionality of the developed software package, as well as conducting experimental studies to improve the parameters of the NFSC by optimizing them, cascading and using integrated technology.

Conflict of interest

The authors declare that there is no conflict of interest regarding the publication of this article.

Funding

The work was carried out with the financial support of the Ministry of Science and Higher Education of the Russian Federation, project FEWM-2023-0014 dated 16.01.2023.

References

1. Malyutin N. D., Trinh T. T., Malyutin G. A. Non-reflective filters (review). *Journal of Radio Electronics. 2024*. No. 4. https://doi.org/10.30898/1684-1719.2024.4.4 (In Russian).

2. Morgan M. A., Boyd T. A. Theoretical and experimental study of a new class of reflectionless filter. *IEEE Transactions on Microwave Theory and Techniques.* 2011. Vol. 59. No. P. 1214-1221.

3. Psychogiou D., Gómez-García R. Reflectionless adaptive RF filters: Bandpass, bandstop, and cascade designs. *IEEE Transactions on Microwave Theory and Techniques*. 2017. Vol. 65. No. 11. P. 4593-4605

4. Wu X., Li Y., Liu X. High-order dual-port quasi-absorptive microstrip coupled line bandpass filters. *IEEE Transactions on Microwave Theory and Techniques*. 2019. Vol. 68. No. 4. P. 1462-1475.

5. Konishi Y., Awai I., Fukuoka Y. Newly proposed vertically installed planar circuit and its application. *IEEE transactions on broadcasting*. 1987. No. 1. P. 1-7.

6. Tripathi V. K. Asymmetric coupled transmission lines in an inhomogeneous medium. *IEEE Transactions on Microwave theory and techniques.* 1975. Vol. 23. No. 9. P. 734-739.

7. Krage M. K., Haddad G. I. Characteristics of coupled microstrip transmission lines-I: Coupled-mode formulation of inhomogeneous lines. *IEEE Transactions on Microwave theory and techniques*. 1970. Vol. 18. No. 4. P. 217-222.

8. Feldshtein A. L. *Synthesis of four-terminal and eight-terminal networks at microwave frequencies* / A.L. Feldstein, L.R. Yavich. 2nd ed., revised. M.: Soviet radio, 1971. – 388 p.

9. Vorobyov P. A. Quasi-T-waves in devices on coupled strip lines with unbalanced electromagnetic coupling / P.A. Vorobyov, N.D. Malyutin, V.N. Fedorov. *Radio engineering and electronics.* 1982. Vol. 27. No. 9. P. 1711–1718.

10. Fusco V. *Microwave circuits. Analysis and computer-aided design*: trans. from English. M.: Radio and Communications, 1990. 288 p.

11. Loschilov A. G., Malyutin N. D., Trinh T. Than. Application of the autonomous blocks method to mathematical modeling of microwave devices containing distributed and lumped circuits. *International Journal of Open Information Technologies*. 2024. Vol. 12. No. 1. P. 61–67. ISSN: 2307-8162.